Atomic Force Microscopy: An Advanced Imaging Technique—From Molecules to Morphologies

5

Jeevan Kumar Reddy Modigunta, Selvamani Vadivel, G. Murali, Insik In, and Montree Sawangphruk

Abstract

Atomic force microscopy (AFM) is an extensively used advanced characterization technique for a nanoscale range of materials. This chapter clearly describes the importance and advantages of AFM, its working principles, modes of measurement, and its applications in interdisciplinary fields such as chemistry, materials science, and biology.

Keywords

Atomic force microscopy · Surface morphology · Sheet thickness · Materials science · Contact mode

The authors Jeevan Kumar Reddy Modigunta and Selvamani Vadivel both contribute equally.

Jeevan Kumar Reddy Modigunta · G. Murali · Insik In (✉)
Department of Polymer Science and Engineering, Department of IT-Energy Convergence (BK21 FOUR), Chemical Industry Institute, Korea National University of Transportation, Chungju, South Korea
in1@ut.ac.kr

Selvamani Vadivel · Montree Sawangphruk
Department of Chemical and Biomolecular Engineering, School of Energy Science and Engineering, Centre of Excellence for Energy Storage Technology, Vidyasirimedhi Institute of Science and Technology, Rayong, Thailand
montree.s@vistec.ac.th

© The Author(s), under exclusive license to Springer Nature Switzerland AG 2022
S.-K. Kamaraj et al. (eds.), *Microscopic Techniques for the Non-Expert*,
https://doi.org/10.1007/978-3-030-99542-3_5

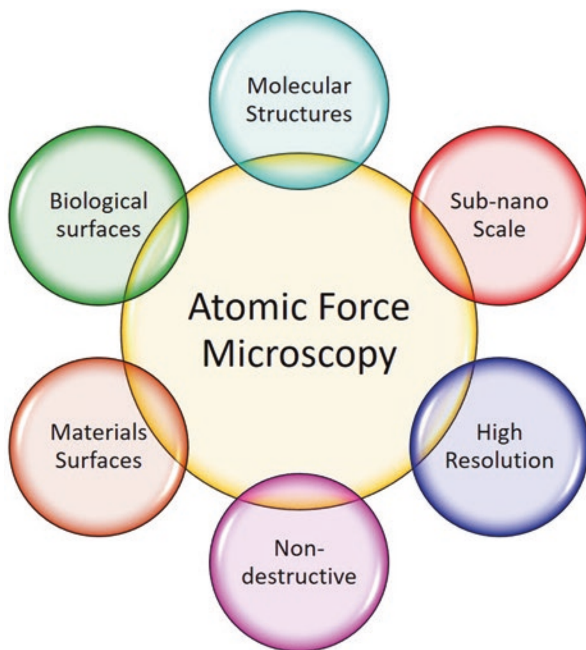

Fig. 5.1 The advantages of atomic force microscopy measurements

5.1 Introduction

The advancement of atomic force microscopy began in 1981 from IBM's researchers on developing scanning tunneling microscopy (STM), as inspired by Russell Young's stylus profiler [1, 2]. Atomic Force Microscopy (AFM) was invented four decades ago by Binnig et al. [3]. In 1987, Wickramsinghe et al. further developed a new AFM setup using a vibrating cantilever technique containing a light-lever mechanism [4]. AFM has become an essential instrument in nanoscience and technology with peculiar abilities to provide three-dimensional imaging at sub-nanometer levels without vacuum or contrast imaging agents [5]. AFM measurement has a broad scope and is more helpful for understanding science and technology in the present era. AFM has been used for the detection of microstructures and surface properties of materials. AFM is used to study various samples such as plastic, metals, glasses, semiconductors, and biological samples (i.e., cells and bacteria walls). It does not require any conductive coatings on the samples' surface as used in STM or scanning electron microscopy. Some of the advantages of AFM are shown in Fig. 5.1.

In comparison to AFM, the optical and electron microscopes can quickly generate 2D (*x*- and *y*-directions) images of sample surfaces with a higher magnification of ~ ×1000 (optical microscope) and ~ ×100,000 (electron microscope), respectively. However, these microscopes fail to measure the sample surface on the third dimension (*z*-direction) by their height (e.g., particles and sheets) or depth (e.g.,

pores). The appropriate AFM probe can scan the surface topology to an extreme magnification of ~ ×1,000,000, which is better than the existing electronic microscopes. Interestingly, the resolution and magnification measured at *z*-direction are usually higher than the *x* and *y* directions.

The rapid advancements of AFM analysis have made notable developments in nanomaterials' characterization in science and engineering. In recent years, there have been many nanomaterials invented and characterized, including graphene. In the past few decades, AFM has been developed majorly in the following aspects:

1. Identifying and revealing more information about the materials at the nanometer level, such as electrical properties, mechanical properties, magnetic properties, surface functionalization, and thermal properties.
2. Easy to combine or integrate with other advanced measurements like optical techniques (infrared, Raman, and fluorescence spectroscopies), molecular characterization techniques (like nuclear magnetic resonance), and so on.
3. Fitting into the life sciences and materials research at different controlled physical parameters (temperature, wet chemical environment, solutions at different pH, illuminating with varying sources of light, and so on).

Based on these advancements in AFM measurements, the application of AFM has further been exploited in interdisciplinary fields for the analyses beyond the topography of materials (semiconductor, polymer, and biological) such as the interfacial interactions, phase transformations at different physical and biological conditions, current vs. voltage characteristics, and defects at the nano-domains of semiconductors.

Depending on the area of interest, different mode of operations is possible in the AFM measurements. Combining AFM with other analyzing techniques like infrared and Raman spectroscopy will achieve a nanometer-scale resolution for the sample analysis. The combination of AFM with other techniques which includes atomic force microscopy-infrared spectroscopy (AFM-IR) [6], atomic force microscopy nuclear-magnetic resonance (AFM-NMR) [7], atomic force microscopy-nuclear rheometer (AFM-Nano-rheology) [8], and atomic force microscope and light-sheet microscope (AFM-LS) [9] were recently developed. Based on the application, the mode of AFM analyses changes such as Bio-AFM for fluid cell enabled contact mode in aqueous solution; dynamic mode AFM (DM-AFM), which oscillates the AFM tip to reduce the friction; and force–distance curve-based AFM (FD-AFM) helps to record pixel-by-pixel measurements at atomic scale for the biological surfaces. Among the various modifications, molecular recognition AFM (MR-AFM) is employed for mapping the specific interactions, especially for biological samples. Multi-parametric AFM (MP-AFM) is used for the mapping of multiple physical or chemical properties. Multi-frequency AFM (MF-AFM) is used for detecting samples while oscillating the cantilever tip at various frequencies to find numerous material properties. Correlation of advanced optical microscope with AFM (Opto-AFM) has been employed for imaging the complex biological systems and a high-speed AFM (HS-AFM) for rapid acquisition of images by a factor of ~1000 to

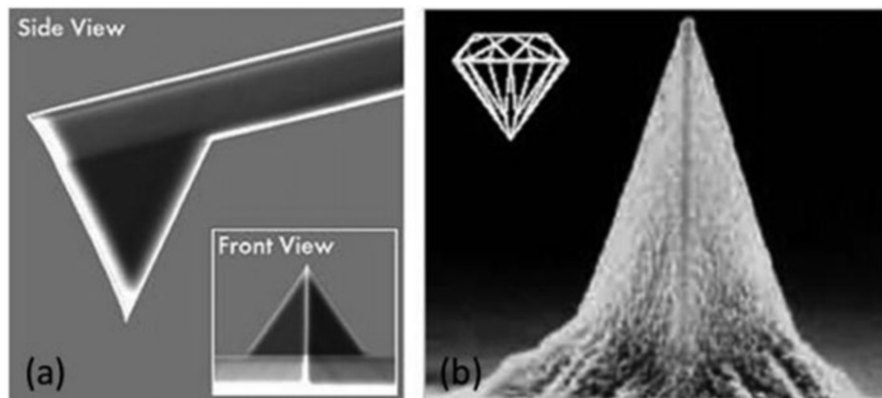

Fig. 5.2 (**a**) The cantilever with silicon nitride (Si_3N_4) tip and (**b**) diamond-coated AFM tip (reprinted with permission from reference [5])

provide access to the dynamic processes in the biological sciences [10]. In this chapter, the authors introduce AFM principles, modes of analysis, different kinds of materials used in the AFM instrument, working methodology, and their applications in detail.

5.2 Principle

AFM works on the combined principles of the Scanning Tunneling Microscope (STM) and the stylus profilometer. In particular, a sharp tip of silicon or carbon mounted on a cantilever spring (Fig. 5.2a) is dragged across the surface of samples with simultaneous feedback system adjustments between the model and tip of the probe. The sharp probe tip runs a raster scan across the sample surface with accurate positioning to the sub-nanometer range. The close feedback loop controls the probe movement to maintain a constant distance between the sample and the tip. The close feedback loop controls the probe movement to sustain a constant distance and a typical forces applied between tip and sample may change from 10^{-11} to 10^{-18} Å. The minimal force required to mobilize the cantilever through a minimum distance can be as small as 10^{-4} N, so the space is discernible, as small as 10^{-4} Å [11]. Therefore, nondestructive imaging of topography is possible without or with minimal damage to the surface of the sample. The surface outline is recorded by monitoring the feedback loop from the photodiode response, which generates the samples' surface topography based on the cantilever deflections.

The commonly used AFM probes consist of a sharp tip and a microcantilever, as shown in Fig. 5.2a. Template-assisted etching methods are usually employed for the fabrication of commercial cantilevers. A silicon wafer was pit etched by masking with desired measurements such as depth of the cavity, width of the recess in a pyramidal shape, or sharp needle type, followed by silicon nitride (Si_3N_4) coating.

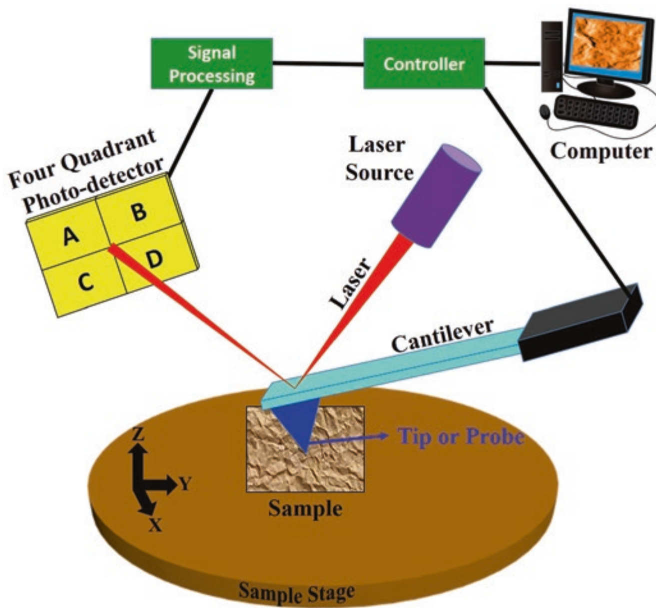

Fig. 5.3 Schematic for the working principle of AFM analysis

Finally, the base silicon substrate was selectively etched to get the desired configuration of the morphology. Several kinds of cantilevers are available based on the application, required sensitivity, and mode of operation. Cantilevers are available in different types such as V-shaped, gold-coated, sharpened needle type, super tip type, and ultra-clever type tips. The diamond-coated tip of the cantilever is shown in Fig. 5.2b. Based on the fabrication process the cantilever tips curvature radius is in the range of a few nm to 30 nm. Most of the microcantilevers are in the range 30–40 μm in width, 125–450 μm in length, and the thickness in the micrometer range to a few micrometers. During the AFM measurement, the laser source used for recording deflections from the cantilever should be highly dense to get an excellent spatial resolution and have very high sensitivity toward the photodiode detector to get a high-quality measurement.

The laser beam directly hits on the surface of the cantilever and reflects towards the mirror. The mirror directly receives the deflected laser beam by the highly sensitive photodetector. The photodiode, a highly-sensitive detector generally used to measure all dimensions as four quadrants (A, B, C, and D) (Fig. 5.3). The A + B detects the UP motion in the four quadrants, and C + D detects the cantilever's DOWN motion. Similarly, A + C sees the LEFT, and B + D detects the RIGHT side motions. Likewise, the deformation or twist in the cantilever will cause a change in the laser beam's position partially on the photodetector. The exact position of the laser beam is determined by using the following process:

The vertical position of the laser is proportional to ((A + B)-(C + D))/(A + B + C + D). Whereas ((A + C)-(B + D))/(A + B + C + D) is proportional to

lateral position. The normalization to the sum signal of (A + B + C + D) is used to eliminate cantilever reflectivity. The optical lever measures the angle of cantilever deflection but not the displacement. Hence, short cantilever probes are more sensitive to detect deflection changes than longer probes. Depending on the cantilever's movement, the photodetector receives the laser beam in different places, and further, they are converted into signals in the processor. The signal processor and cantilever are connected to the control unit, which further joined with the computer to convert signals into images and data. The detailed schematic, working principle of the AFM analysis is shown in Fig. 5.3.

The AFM scanners have horizontal and vertical movements in *XY* and *Z* dimensions. The sample stage in AFM has a piezoelectric scanner that determines the sample's position by nanometer scale, where the high voltage drives the *XYZ* directional movements in multiples of hundreds. The distorted AFM images are recorded during the piezo scanner's nonlinear motion while applying the steady voltage, whereas the piezoelectric materials do not respond to the applied voltages. The modern AFM instruments are equipped with *XYZ* position monitoring sensors, and the nonlinearity of the voltage is rectified by using a closed feedback loop. For more accuracy in the measurements, the voltages are tuned until the scanner reaches the desired position and it is called as closed-loop method [12].

The other procedure is an open-loop method, in which the nonlinearity is first adjusted then followed by the nonlinear voltage to drive the scanner to get the linear movement. A standard grid image was taken for calibration using different scan rates, scan sizes, and scan angles in this procedure. Finally, after finishing the scans and parameter corrections, the scanner movement against the applied voltage and scan conditions is obtained by fitting the data. This open-loop method is more beneficial to get a good high-resolution image. But this process is vulnerable to the position sensors and noise of the instrument. The sensors research development has helped to develop different sensors for different positions in AFM instruments such as optical sensors, capacitive sensors, strain gauge, and inductive sensors to overcome the sensitivity issues and get more accurate measurement. Therefore, in all the AFM measurements, by utilizing the combined effort from the sensor technology, high-resolution imaging is carried out using the closed-loop method instead of the open-loop method.

The deflection sensitivity of the cantilever is determined by its length and the sensitivity of the photodetector. For better reproducibility and precise measurements, the incident point and the approach/retract turning point are usually excluded from the calculation. The cantilever's short length is more preferred for obtaining high sensitivity during measurement of displacement in the pm range. The cantilever's effective length and laser position realignments will determine the deflection sensitivity due to laser spot position change. In general, the deflection sensitivity must be measured for every single AFM measurement due to the laser beam's realignment. The deflection sensitivity is calibrated by calculating the change in deflection of the cantilever from the voltage deflection. For a cantilever with a rectangular cross-section, the spring constant (k) can be expressed as:

$$k = \frac{Et^3 w}{4L^3}$$

Here, E is Young's modulus of the cantilever material (silicon or silicon nitride), t, w, and L are the thickness, width, and length of the cantilever, respectively. The k value is different for each cantilever as there may be a slight change in the cantilever's manufacturing process through microfabrication techniques. The thickness of the cantilever can be controlled by careful fabrication, but a minimum of 10% thickness error can cause an error in the spring constant three times. But in usual practice, the value given by the manufacturer is used for further calculations. The cantilevers must be calibrated before recording to get an accurate force value. The easy method to measure the spring constant (k) value is by using the following formula.

$$k = bf^3$$

Where resonance frequency (f) of a probe and b is the probe factor from the references. The direct measurement of the resonance frequency is by "auto-tune" in tapping mode analysis of AFM. But this method has poor accuracy due to the slight changes in the cantilever's dimension than as shown in reference value. The other way for calculating the resonance frequency of the cantilever is using the formula:

$$f = \frac{1}{2\pi}\left[\frac{k}{m_0}\right]^{0.5}$$

where k is the spring constant, m_0 is the effective mass of the lever. The toughness of the leveler is also an essential aspect in the calculation of resonance frequency. The leveler's softness is inversely proportional to the spring constant and directly proportional to the sensing of the deflection on the samples' surface [13]. But the cantilever must be smaller to keep the frequency higher for the detection of vibrations during the analysis. After several modifications and considering the different variables, finally, in the modern methods of AFM instrumentation, the cantilever's thermal noise has been used to calculate the spring constant and considered reliable [14]. The spring constant formula is as follows:

$$k = k_B T / z^2$$

where k_B and T are Boltzman constant = 1.3805×10^{-23} Joule/Kelvin and absolute temperature in Kelvin, respectively. Almost all AFM instruments with automatic software use this method, whose frequency ranges are from a few kHz to 2 MHz.

5.3 Working

In AFM, the cantilever/tip assembly plays a vital role and is often referred as a probe, which governs data interaction and quality. The tip's substrate is typically made of silicon/silicon nitride which is different from the cantilever material. Each material has its advantages; for instance, silicon-based materials are used to

fabricate sharp tips. The tip shape and size or radius at the apex are more critical, which defines the quality and range of operations. The corrugated AFM nail limits an image's resolution substantially on the lateral side of view due to the large surface area.

The AFM probes fabrication is a tedious method in the earlier days and made with a diamond shard by gluing to the thin metallic foil or wire (as a cantilever made up of Fe, W, or Ni). The first commercial AFM probe consists of Si_3N_4 thin film coated on the glass substrate as a cantilever and the square pyramidal-shaped tip with an apex of the radius of curvature about 20 nm. Such pyramidal AFM tips offer an opening apex angle of 60–70°. The AFM probe tips are customizable, and the generation has evolved into several types depending on the applications. For ambient and vacuum analysis, the monolith types of probes are more appropriate, especially monolithic silicon, fabricated from the Si wafer through etching. A diamond tip glued cantilever is also commercially available for high wear resistive, stable shape imaging, and more reliable electrical measurements. In addition to the sharp-edged tip, the round-headed apex with a large surface of 50–100 nm was also deployed for nano-mechanical measurements and low wear imaging. Off-late, owing to the high flexibility of AFM tip, the surface modification or coating has been introduced, especially for the study of chemical and biological applications. For example, the gold-coated tip provides better imaging for biological samples through gold–thiol interactions. Similarly, the cobalt or platinum-coated tips offer a good platform for electric or magnetic property measurements.

5.4 Sample Preparation and Handling

The experiment of AFM starts with sample preparation, probe selection, and microscope settings. More attention needs to pay while imaging the artifacts, which appear as substantial contrast change or identical structures as islands. Several factors influence such artifacts including, sample surface contamination, AFM tip condition, and shape. Therefore, it is highly advisable to store the samples under controlled conditions before the analysis. The AFM tip apex is vulnerable to damage on interaction with bulk samples, and hence additional care should be taken.

The AFM imaging requires:

1. Solid and rigid adherence of samples to the substrate to avoid their displacement by the probe.
2. Good dispersion.
3. The surface roughness should be lower than the sample particle size.

The substrate choice is not limited; however, the glass slide, freshly cleaved mica, or HOPG surface are commonly used. The polymeric adhesives are often required to affix the nano-sized samples to the substrate, facilitating strong particle-to-substrate affinity than the tip-to-substance interactions. The most common binders are poly-D-lysin, poly-L-lysin, poly-ethyleneimide (PEI), and

aminopropyltriethoxy-silane (APTES) improve adhesive property thru chemical bonding [15]. For fine powders (<150 nm), the uniform distribution is achieved via the dusting method followed by flipping and gentle tapping to remove the agglomerated particles. Similarly, the drop-casting process also provides good images. The sample is prepared by dispersing in alcohol/toluene/water (0.1 mg/ml) and deposited over the glued substrate or freshly peeled mica substrate [16]. Before scanning, the sample should be dried at ambient or accelerated heating under dust-free conditions. In the case of larger granular particles (>500 nm), a polished metal substrate with thermal wax glue offers a better platform for scanning. The sample preparation and imaging also be a big challenge, especially for biological samples owing to the low elastic modulus is in the range of kPa, for cells. However, some of the macromolecules and bone-type materials display significantly higher elastic modulus in GPa. Although special conditions are required for those samples due to wetness and softness, the AFM probe extends its application to study the variation of local surface charge, hydrophobicity, and nano-mechanical properties. Extreme care should pay in case of bio-sample to meet the essential requirement of substrate flatness and chemical compatibility through mechanical trapping and non-covalent physisorption. Not only powders but also biological cell samples are prepared by dispersion-evaporation, spray drying, and dip coating methods over the freshly cleaved mica substrate. Further, to improve the strong binding, chemical functionalization (i.e., Salinization) is applied to those samples.

5.5 Modes of AFM Analysis

The mode of AFM operations are broadly classified into two types such as contact or static and dynamic mode. The latter has further been subdivided into intermittent contact or tapping (standard or soft) and noncontact modes (as shown in Fig. 5.4).

In detail, the contact AFM mode is also known as a repulsive or static mode of operations, where the tip of the cantilever is in perpetual contact with the sample surface. The cantilever's spring constant must be lower than the effective spring

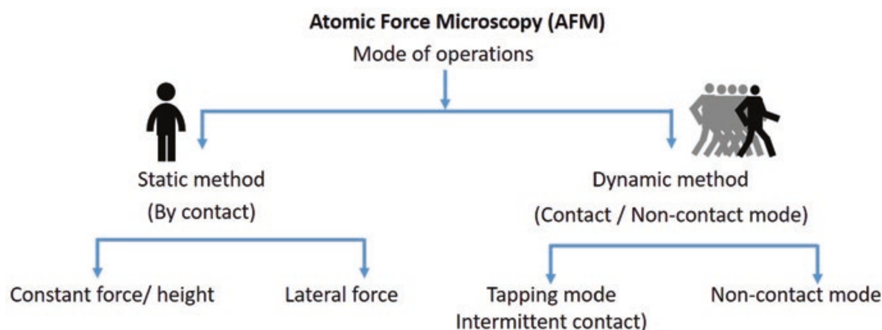

Fig. 5.4 The classification of fundamental modes of operations in atomic force microscopy

constant of atom–atom interactions in solids. This method is mainly used to image the hard surfaces to get a molecular or atomic level resolution of crystalline substrates. During the operation, the tip gently scans across the surface. The interaction or contact force between the sample and AFM tip is calculated from the cantilever's force constant and its deviation. Generally, a constant force or deflection feedback mode is used to measure such repulsive interactions, which vary from sub-nano to a few micro newtons in range. The AFM feedback systems are more sensitive to detecting such deflection. A piezo-actuator is usually employed to minimize the cantilever deflection by retracting the AFM probe (by vertical *x*-*y* movement) and maintaining a constant deflection, which further helps to retain the force between the tip and sample remains the same. The repulsion force F experienced by the AFM-tip is directly related to the cantilever deflection value *x* and calculated from Hook's law:

$$F = -kx$$

where *k* is spring constant. At ambient conditions, on this side, the initial large force typically from ten to a hundred nano-Newtons between the tip and sample damage or deform the surface of soft materials.

On the other side, the sample's rigid texture destroys the tip apex's sharpness during operations' contact mode. The probe with soft cantilevers <1 N/m is preferable to achieve high deflection sensitivity while keeping the interaction force is significantly low. The cantilever's length also plays a vital role, which varies from a few tens of micrometers to several hundreds, usually 400–500 μm; however, the shorter length offers higher sensitivity, while the materials have the same force constant.

A constant height mode of scanning can also be performed under static conditions to get atomic resolution by maintaining the probe at a fixed height. In such cases, no feedback force has been applied to the probe. Such high-resolution imaging can only be achieved for smooth samples. This method's significant advantage is high-speed scanning; however, it is limited to the cantilever's resonant frequency. Besides, it also has some drawbacks while scanning the soft materials, for instance, soft polymers, bio-samples, etc., which destroy the sample by scratching due to the proximity of tip and sample. In this contact AFM method, the soft cantilever's tip is susceptible to distort the image features by lateral or shear forces and the surface contaminants, especially in the ambient air atmosphere. The initial high pressure and the lateral shear force tend to suppress the spatial resolution and damage the soft sample by scrapping. The detailed cantilever deflection and modes of operation are shown in Fig. 5.5.

In contact mode of operation, lateral force imaging is also performed, where the cantilever deflection is in a horizontal direction, which is controversial to the conventional vertical movement. The characteristic of the change in samples' surface friction can be gauged using this method by measuring the interaction between the tip and sample, resulting in lateral bending or twisting of the cantilever. The lateral deflection arises by the change in frictional coefficient of a sample via the applied force to the cantilever during the lateral scanning.

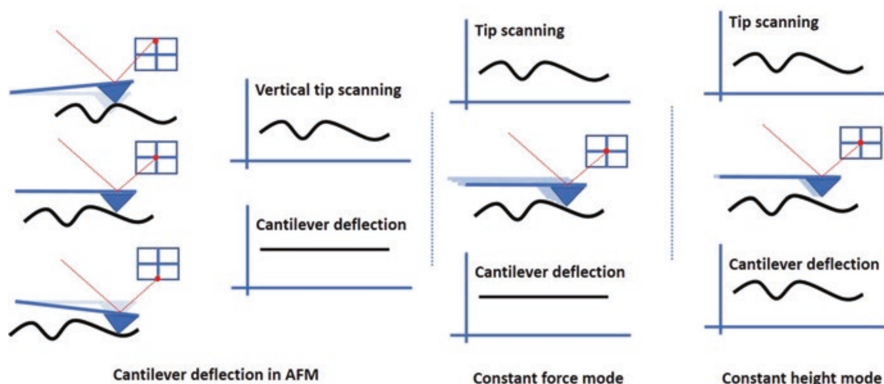

Fig. 5.5 Cantilever deflection and types of static mode of operations in AFM

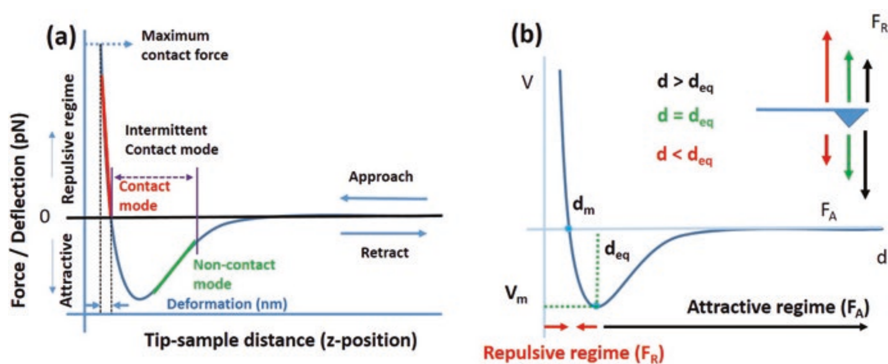

Fig. 5.6 (**a**) Force–distance curve and (**b**) Lennard–Jones potential plot of nonbonding interactions at different circumstances

It is challenging to choose the mode of imaging for individual samples in advance; however, the deflection vs. distance, i.e., force curve measurements between the models to tip, guides to select the appropriate test condition and the probe (as shown in Fig. 5.6a). The elastic and inelastic deformation force between the AFM tip-sample capillary or adhesion can easily be distinguished using the force curve. In specific, if the tip-sample distance is well pronounced, then the resultant force is Van der Waals attractive. On the other hand, the close-enough space leads to strong repulsion (Pauli's) due to orbital overlapping. The approximate force can be calculated using the Lennard-Jones potential graph (Fig. 5.6b), which describes the interaction between nonbonding atoms as a function of distance:

$$V(d) = 4V_m\left[\left(\frac{\mathrm{d}_m}{d}\right)^{12} - \left(\frac{\mathrm{d}_m}{d}\right)^{6}\right]$$

$V(d)$ is intermolecular potential. V_m is well-depth, and a measure of attraction between the particles, d-particle separation from the center, and d_m distance at $V = 0$, i.e., how close the two nonbonding particles and referred to as van der Waals radius. As the separation distance is equal to the equilibrium distance ($d = d_{eq}$), the resultant force is zero on the tip until the external force is applied. Suppose the tip-sample space is below the equilibrium distance ($d < d_{eq}$) the consequent potential energy increases due to the atomic orbitals overlapping (repulsive force, $F_{R,}$ is dominant). On the contrary, the significant separation between the tip and sample, $d > d_{eq,}$ displays high negative potential and tends to reach equilibrium, indicating the existence of robust, attractive force [17].

The feedback acquisition should be high under an optimized scanning rate to record a stable AFM image, which could be achieved by setting a low deflection set point to minimize the tip-sample force. The selection of soft AFM cantilevers could also overcome excessive force. Similarly, other interference forces such as capillary or meniscus and other attractive forces that arise from the monolayer adsorption of water vapor/gas molecules could be neutralized by the complete immersion in liquids.

In the noncontact mode of imaging, the AFM tip is hungover (~50–150 Å) to scan the topographic image by a smaller amplitude of the cantilever's oscillation (<10 nm). Typically, the interaction between tip and sample is attractive van der Waals force, which is substantially weaker than that of the force used in the contact mode of operations. This method's main advantage is to achieve high-resolution images due to poor possible interaction with the sample surface, which retains the tip's sharpness, especially in extreme hydrophobic samples. However, it is not that easy to preserve the AFM tip in the van der Waals regime. The slow-scan imaging, the poor lateral resolutions, and the attractive gradient force due to the thick fluid contaminants hampered such a noncontact mode of operation. Such limitation has been suppressed by employing a high-performance feedback controller, ultra-high vacuum chamber, etc.

In the dynamic mode, the Tapping method is a widely employed and more effective method to scan the sample while comparing it to the noncontact AFM imaging. It overcomes some of the problems and limitations associated with other modes of AFM operations, including destructive frictional force, electrostatic interference, capillary interaction, and adhesion. Herein, the probe is associated with a piezoelectric transducer to oscillate the cantilever near the resonance frequency (10 – a few 100 kHz) to sense long-distance van der Waals forces (both attractive and repulsive force regimes). During the operation, the lower end of the AFM tip is close to the sample and record the damping oscillation amplitude, which is typically in the range greater than 20 nm. Upon scanning, the AFM tip experiences intermittent contact with the models by vertical oscillation, and the frequency range is 50–500 k cycles per second. In this mode, either the cantilever's oscillation amplitude or phase change is used in a feedback loop to maintain a constant probe-sample distance by z-axis movement, which is the direct measurement of sample height (Fig. 5.7).

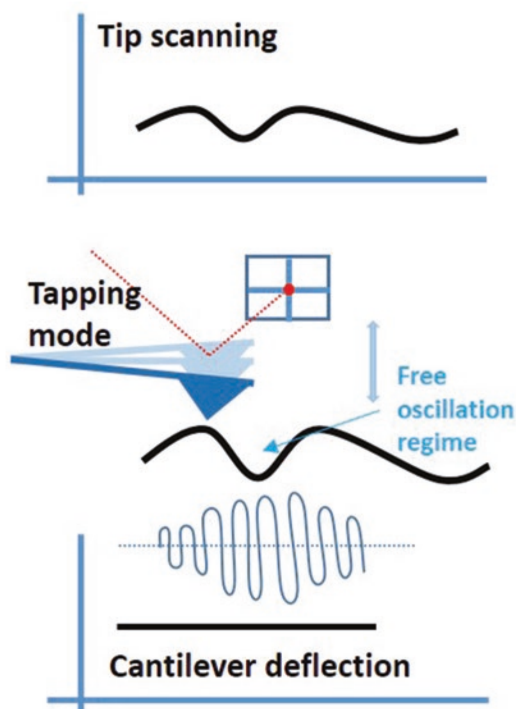

Fig. 5.7 Dynamic tapping mode of AFM operation

On the sample surface, the oscillation amplitude decreases, whereas, at the depression point, it reaches maximum owing to more space for probe the swinging. The tapping mode of scanning is less destructive and preferable, where the high frequency of oscillation significantly reduces the adhesion force between the tip and samples due to viscoelastic stiffness. The significant difference between the non-contact and tapping mode of dynamic operation is the AFM tip placement during the probe oscillation; in the former case, the tip stays only at the attractive Van der Waals regime, whereas such control extends into the repulsive force region in the tapping mode. In practice, the probe's lower force constant minimizes the immense tip-sample attraction to oscillate freely, typically in the range of a few tens of N/m. Besides, this technique offers high lateral resolution images (1–5 nm) with significantly less or no damage to soft samples. However, the speed of scanning is slower compared to the contact mode of imaging. Not surprisingly, the soft Si probe is widely applied for tapping mode of operation at ambient air conditions, also providing a good image in fluid media. Generally, wide-ranging resonance frequencies are more desirable to acquire complete scanning faster; however, the standard probe used in the dynamic mode of AFM operation is limited and requires distinctive geometries.

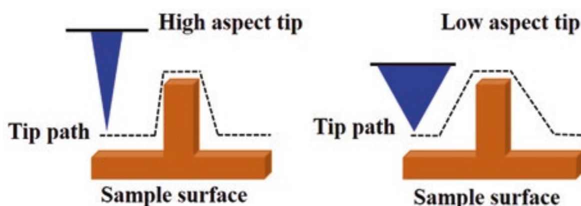

Fig. 5.8 The probe or tip with a high aspect ratio will provide a high resolution. The probe with high radius curvature results in a low aspect ratio due to tip convolution. In both cases, the height of the sample is not affected, but the resolution of the image drastically varies

5.6 Factors Affecting AFM Imaging

The quality of the AFM image depends on several factors; however, the tip shape and the apex's radius of curvature play a significant role. In contrast to the sharp apex, the broad and dull tip edge fails to scan the sample's more minor features. For example, a larger tip size will result in a more prominent feature size than its original or the actual size, and it cannot differentiate between two or more adjacent features of the samples. Therefore, a sharp tip cantilever is required. The debris accumulated over the edge also distorts the image quality. Imaging small features and scanning small areas at high resolution requires ultra-sharp tips. However, the commercial probes with very high aspect ratios are widely available, made with materials such as carbon nanotubes or tungsten spikes. These kinds of costly probes are still an unresolved issue for everyday usage of AFM analysis. To achieve a high atomic resolution, using an appropriate ideally sharp probe is needed. The probe-to-sample interaction at the surface must be improved by modifying the surface morphology and/or functional groups, and dimensions of the probe (Fig. 5.8).

5.7 Applications

AFM, a powerful imaging tool to study nano and sub-nano level scale surface morphologies in the broad discipline of materials, including semiconductor technology, surface chemistry of thin-film, polymer coatings, molecular as well as cell biology, piezoelectric, and ferroelectric properties. Among all these studies, let us consider the molecules and morphologies for easy understanding.

5.7.1 Molecules

Biomolecule structure imaging is not accessible due to their poor sensitivity that deviates from the average molecular structures. The bimolecular designs can be determined using the soft-touch AFM in combination with the image analysis method. By this method, many molecules and highly complex and basic structures can also be studied. Figure 5.9 describes the AFM images of double-helical

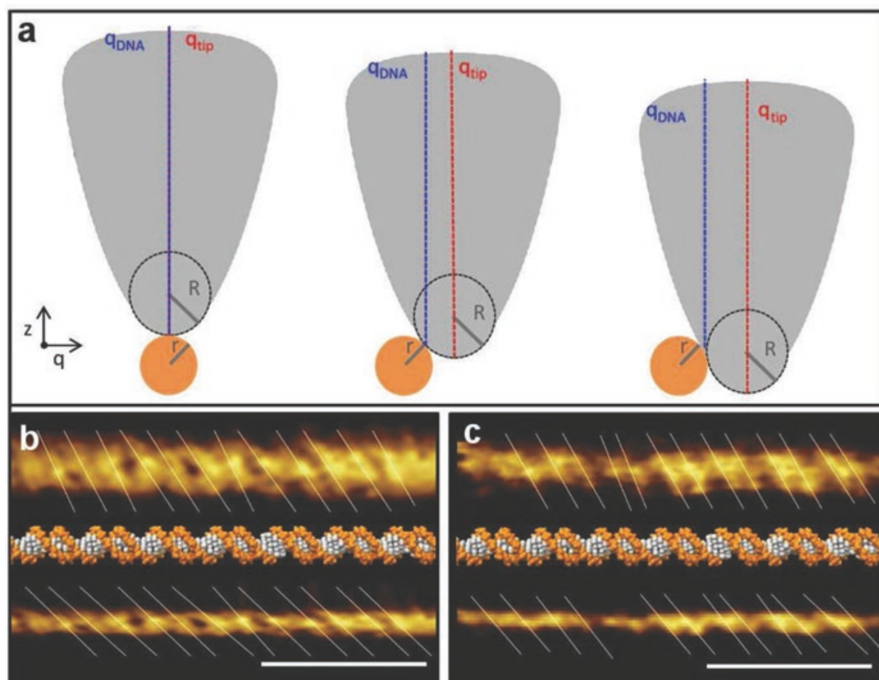

Fig. 5.9 The chiral angle measurement of the double helix of DNA using AFM. (**a**) Schematic for the AFM tip with radius *R* at different positions on the surface of DNA sample with radius *r* (cross-sectional view for easy understanding). (**b**, **c**) The AFM topography of digitally straightened parts of DNA before (top) and after (bottom) correcting with a definite tip size in comparison with the B-DNA crystal structures. (**b**) $r = 1.1 \pm 0.1$ nm, $R = 1.3 \pm 0.2$ nm, and (**c**) $r = 0.9 \pm 0.1$ nm, $R = 1.7 \pm 0.2$ nm. Scale bars: 10 nm; reprinted with permission from reference Pyne et al. [18]

DNA. This combination of AFM with image analysis technique is more helpful in understanding the biological complex molecules [18, 19].

The asphaltene's complex structure has been imaged using AFM with functionalized tip, as shown in Fig. 5.10. Coal-derived asphaltene (CA) sample preparation for the analysis is shown in Fig. 5.10a, and CA molecular structure is characterized using AFM at different distances. Currents are shown in Fig. 5.10b–g. The asphaltene's molecular structure is visible at the sample to tip distance of −0.9 Å using AFM analysis, as shown in Fig. 5.10c. The STM analysis of the CA sample at different currents is shown in Fig. 5.10e, f. From this analysis, AFM measurement has resulted as a replica of CA's chemical structure is seen compared to STM analysis.

An indispensable metrology technique of AFM is used in the semiconductor field to characterize the trenches and holes present in the high-performance microelectronic circuits. The integrated circuit matrix's topography and electric properties have been studied by combining the Kelvin force probe and scanning capacitance probe with conductive AFM. Besides, such nanoprobe technique helps to

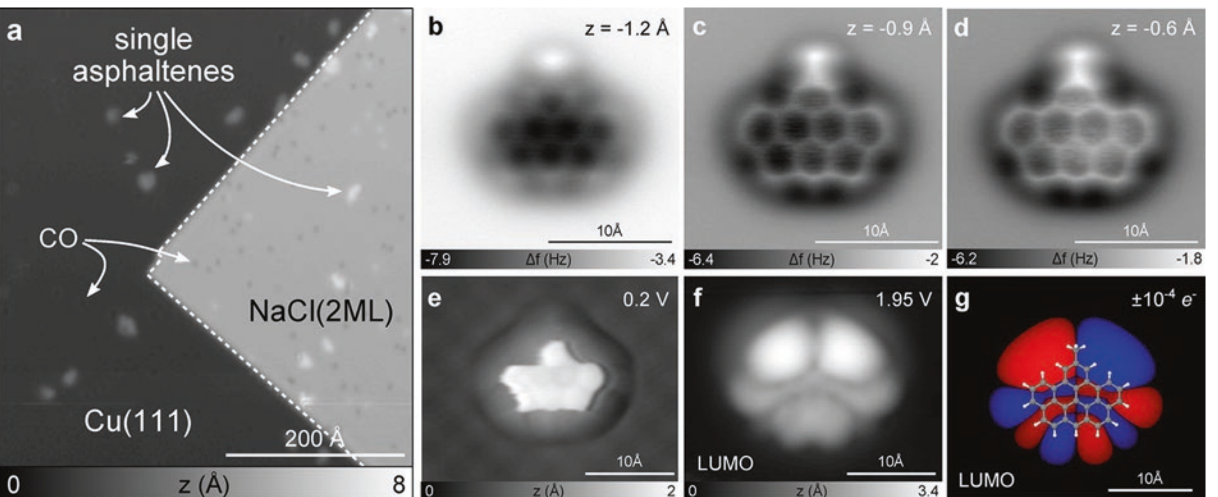

Fig. 5.10 (**a**) Coal-derived asphaltene (CA) sample preparation and analysis. Scanning tunneling microscopic overview image of the CA sample on NaCl(2 ML)/Cu(111) substrate prepared using a flash evaporation process. (**b–d**) AFM images of CA on NaCl(2 ML)/Cu(111) at different set-points z from (I = 1.4 pA, V = 0.2 V). (**e**) STM image of CA (I = 10 pA, V = 0.2 V). (**f**) STM image at the NIR (I = 1.4 pA, V = 1.95 V). (**g**) LUMO orbital of CA with the molecular structure overlaid as a guide to the eye. CO-functionalized tips have been used for all AFM and STM measurements shown (reprinted with permission from reference Schuler et al. [20])

investigate the localized failure, mainly invisible soft failure in memory chips due to complex layout.

In material chemistry, especially energy storing lithium-ion batteries, the localized lithium concentration has been studied during cycling by integrating with a Raman spectrometer. AFM helps to understand the evolution and degradation of solid electrolyte interfacial layer formation over the electrode, especially anode by operando and in situ measurements [21]. The localized electrical, mechanical properties, aging effects, and other limiting factors of the cathode include inactive localized area, surface contaminants (either physisorbed or chemisorbed), reaction products, etc. Mechanical properties of thick electrodes used in high-energy batteries are crucial, especially to retain the integrity of stiffness and elastic modulus; hence contact-resonance, frequency, or amplitude modulation AFM methods is employed for investigation. The contact-resonance AFM (CR-AFM) is a static contact mode of operation and susceptible to tip damage. In contrast, frequency or amplitude modulation is a dynamic nondestructive tapping mode of scanning and offers high-resolution images. The bulk electrode's surface conductivity has been investigated with a conductive probe AFM, where the Kelvin probe provides to measure the surface potential at micro to the nanoscale level.

The AFM also provides high-resolution real-time 3D images (both vertical and lateral imaging) for biological samples, although it is probe selective. This technique helps to study the micromechanical properties of biosamples such as surface properties, viscoelastic nature, Young's modulus, adhesion, mechanical, and friction forces. In contact mode, soft probes are preferable for macro-biomolecules, where the stiffness is ≤ 0.1 N/m, for instance, soft silicon probe, etc. Besides, biologic samples offer reduced interference under the liquid immersed condition, especially in buffered media. Off-late, the AFM analysis extends its application to perform the nondestructive imaging of living cell's membrane, especially membrane protein, lipids, and their interactions. The amplitude modulation or frequency modulation method of AFM offers high-resolution bio-images both in ambient and vacuum conditions.

5.7.2 Morphologies

The surface morphologies of the biological and inorganic materials can be easily studied using AFM analysis. The dimensions of the samples were also understood using AFM analysis. In the biological system, the major components of the human blood collected from a healthy donor i.e., platelets and erythrocytes were analyzed in air. Figure 5.11a, c are height images, whereas (b) and (d) are error signal images.

The surface profiling of the inorganic MXene ($Ti_3C_2T_x$) sheets using AFM analysis provides a clear understanding of the prepared MXene sheets' thickness and size [23]. The AFM image of MXene nanosheets is shown in Fig. 5.12. The height profile describes the synthesized MXene as multilayer in structure with an average thickness of ~200 nm.

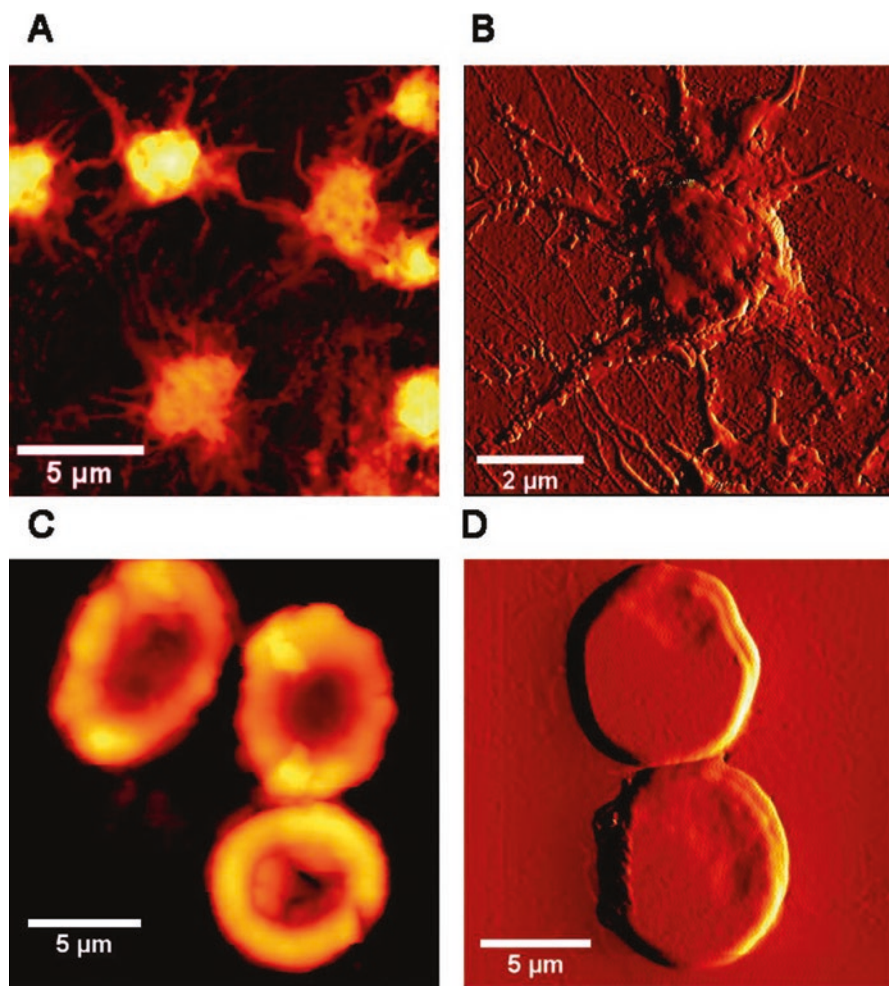

Fig. 5.11 AFM imaging in air of human platelets (**a**, **b**) and erythrocytes (**c**, **d**) from healthy donors. (**a**) and (**c**) are height images, whereas (**b**) and (**d**) are error signal images (reprinted with permission from reference Carvalho et al. [22])

The surface depth profile and pore size were analyzed for the honeycomb patterned porous polymer films fabricated using the breath-figure method [24]. The porous structures were differentiated in AFM analysis depending on the morphology of the polymer films. Single-layer pores and multilayers pores were distinguished, as shown in Fig. 5.13.

In summary, AFM is one of the advanced techniques used for the recording and analysis of the topology of the materials, and the molecular structures of the materials. There is no other technique having the capability of direct molecular structure imaging. Combining AFM with other procedures like IR, NMR, and other optical instruments is an added advantage for characterizing the rare phenomenons

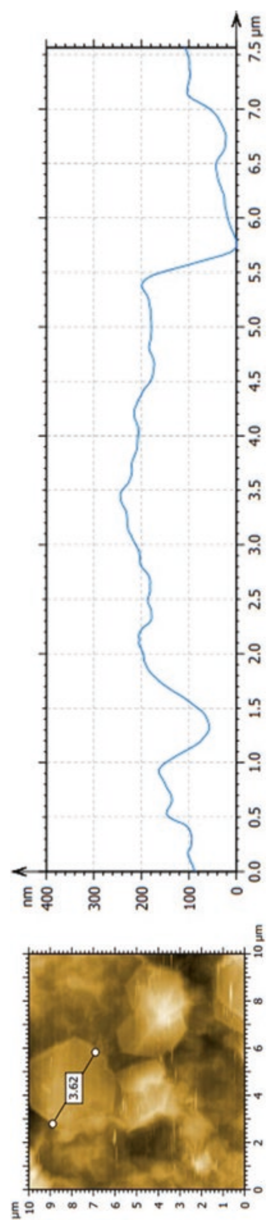

Fig. 5.12 AFM analysis of MXene flakes by contact mode with sheet thickness of ~200 nm and 3.62 µm size

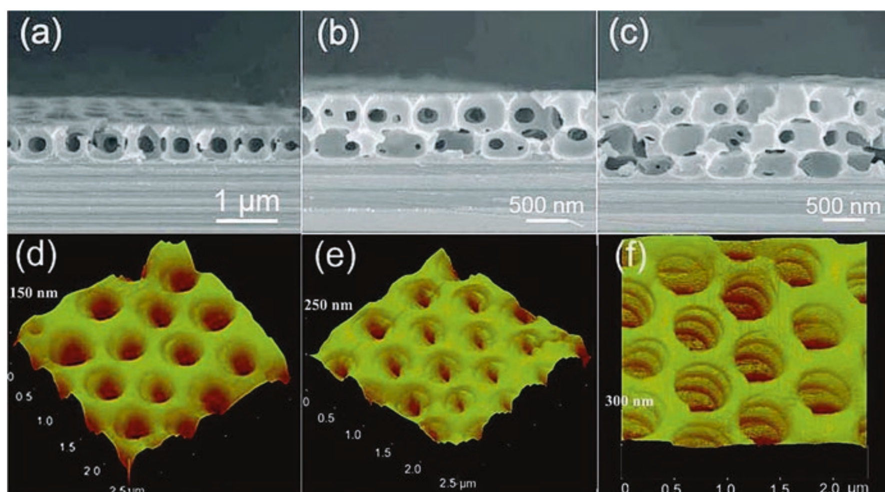

Fig. 5.13 Honeycomb patterned porous polymer films fabricated using breath figure method by dissolving polymer material in carbon disulfide solvent and cast on a silicon substrate. (**a**–**c**) Cross-sectional SEM images of the single, double, and multilayer porous structures. (**d**–**f**) Three-dimensional AFM images with depth profile (reprinted with permission from reference Dong et al. [24])

in science and engineering. The biological samples are easily studied without any damage using the AFM method. AFM is one of the best nondestructive techniques without using any conductive additive on the samples' surface for the analysis. AFM is the best tool to understand the polymer systems' interfacial phenomenons, a biological system's bioimaging with high-resolution capability ~100,000 times that of other techniques. Further modification of probes used like change in the cantilever's size and shapes, surface modification of the probe tips using gold or diamond coatings helps get the samples' better resolution and accuracy using AFM analysis. Further improvements and changes by addressing the present issues in AFM can become a powerful tool for understanding many unknown phenomenons in science and technology.

Acknowledgments This research was supported by the Radiation Technology R&D program (NRF-2017M2A2A6A01019289), funded by the Ministry of Science, ICT and Future Planning. This research was supported by the Basic Science Research Program through the National Research Foundation of Korea (NRF), funded by the Ministry of Education (2018R1A6A1A03023788 and 2021R1I1A1A01055790). Additionally, this work was supported by the Korea Institute for Advancement of Technology (KIAT) grant funded by the Korean Government (MOTIE) (P00008500, The Competency Development Program for Industry Specialist). This work was supported by the Material Components Global Investment Linkage Technology Development Project (Global Open Technology Development Project) (20013593) of the KEIT, MOTIE (KOREA).

References

1. Binning G, Rohrer H, Gerber C, Weibel E (1993) Surface studies by scanning tunneling microscopy. In: Neddermeyer H (ed) Scanning tunneling microscopy. Springer, Dordrecht, pp 31–35. https://doi.org/10.1007/978-94-011-1812-5_1
2. Young R, Ward J, Scire F (1972) The Topografiner: an instrument for measuring surface microtopography. Rev Sci Instrum 43(7):999–1011. https://doi.org/10.1063/1.1685846
3. Binnig G, Quate CF, Gerber C (1986) Atomic force microscope. Phys Rev Lett 56(9):930–933. https://doi.org/10.1103/PhysRevLett.56.930
4. Martin Y, Williams CC, Wickramasinghe HK (1987) Atomic force microscope–force mapping and profiling on a sub 100-Å scale. J Appl Phys 61(10):4723–4729. https://doi.org/10.1063/1.338807
5. Nguyen-Tri P, Ghassemi P, Carriere P, Nanda S, Assadi AA, Nguyen DD (2020) Recent applications of advanced atomic force microscopy in polymer science: a review. Polymers 12(5). https://doi.org/10.3390/polym12051142
6. Dazzi A, Prater CB (2017) AFM-IR: technology and applications in nanoscale infrared spectroscopy and chemical imaging. Chem Rev 117(7):5146–5173. https://doi.org/10.1021/acs.chemrev.6b00448
7. Mousoulis C, Maleki T, Ziaie B, Neu CP (2013) Atomic force microscopy-coupled microcoils for cellular-scale nuclear magnetic resonance spectroscopy. Appl Phys Lett 102(14):143702–143702. https://doi.org/10.1063/1.4801318
8. Lherbette M, dos Santos Á, Hari-Gupta Y, Fili N, Toseland CP, Schaap IAT (2017) Atomic force microscopy micro-rheology reveals large structural inhomogeneities in single cell-nuclei. Sci Rep 7(1):8116. https://doi.org/10.1038/s41598-017-08517-6
9. Hobson CM, Kern M, O'Brien ET, Stephens AD, Falvo MR, Superfine R (2020) Correlating nuclear morphology and external force with combined atomic force microscopy and light sheet imaging separates roles of chromatin and lamin A/C in nuclear mechanics. bioRxiv:2020.2002.2010.942581. https://doi.org/10.1101/2020.02.10.942581
10. Dufrêne YF, Ando T, Garcia R, Alsteens D, Martinez-Martin D, Engel A, Gerber C, Müller DJ (2017) Imaging modes of atomic force microscopy for application in molecular and cell biology. Nat Nanotechnol 12(4):295–307. https://doi.org/10.1038/nnano.2017.45
11. Maghsoudy-Louyeh S, Kropf M, Tittmann BR (2018) Review of progress in atomic force microscopy. Open Neuroimaging J 12:86–104. https://doi.org/10.2174/1874440001812010086
12. Kenkel S, Mittal S, Bhargava R (2020) Closed-loop atomic force microscopy-infrared spectroscopic imaging for nanoscale molecular characterization. Nat Commun 11(1):3225. https://doi.org/10.1038/s41467-020-17043-5
13. Shao Z, Mou J, Czajkowsky DM, Yang J, Yuan J-Y (1996) Biological atomic force microscopy: what is achieved and what is needed. Adv Phys 45(1):1–86. https://doi.org/10.1080/00018739600101467
14. Horcas I, Fernández R, Gómez-Rodríguez JM, Colchero J, Gómez-Herrero J, Baro AM (2007) WSXM: a software for scanning probe microscopy and a tool for nanotechnology. Rev Sci Instrum 78(1):013705. https://doi.org/10.1063/1.2432410
15. Engel A, Müller DJ (2000) Observing single biomolecules at work with the atomic force microscope. Nat Struct Biol 7(9):715–718. https://doi.org/10.1038/78929
16. Vesenka J, Manne S, Giberson R, Marsh T, Henderson E (1993) Colloidal gold particles as an incompressible atomic force microscope imaging standard for assessing the compressibility of biomolecules. Biophys J 65(3):992–997. https://doi.org/10.1016/S0006-3495(93)81171-8
17. Stylianou A, Kontomaris S-V, Grant C, Alexandratou E (2019) Atomic force microscopy on biological materials related to pathological conditions. Scanning 2019:8452851. https://doi.org/10.1155/2019/8452851
18. Pyne A, Thompson R, Leung C, Roy D, Hoogenboom BW (2014) Single-molecule reconstruction of oligonucleotide secondary structure by atomic force microscopy. Small 10(16):3257–3261. https://doi.org/10.1002/smll.201400265

19. Gross L, Mohn F, Moll N, Liljeroth P, Meyer G (2009) The chemical structure of a molecule resolved by atomic force microscopy. Science 325(5944):1110. https://doi.org/10.1126/science.1176210
20. Schuler B, Meyer G, Peña D, Mullins OC, Gross L (2015) Unraveling the molecular structures of asphaltenes by atomic force microscopy. J Am Chem Soc 137(31):9870–9876. https://doi.org/10.1021/jacs.5b04056
21. Lang S-Y, Shi Y, Hu X-C, Yan H-J, Wen R, Wan L-J (2019) Recent progress in the application of in situ atomic force microscopy for rechargeable batteries. Curr Opin Electrochem 17:134–142. https://doi.org/10.1016/j.coelec.2019.05.004
22. Carvalho FA, Connell S, Miltenberger-Miltenyi G, Pereira SV, Tavares A, Ariëns RAS, Santos NC (2010) Atomic force microscopy-based molecular recognition of a fibrinogen receptor on human erythrocytes. ACS Nano 4(8):4609–4620. https://doi.org/10.1021/nn1009648
23. Murali G, Rawal J, Modigunta JKR, Park YH, Lee J-H, Lee S-Y, Park S-J, In I (2021) A review on MXenes: new-generation 2D materials for supercapacitors. Sustainab Energy Fuels 5(22):5672–5693. https://doi.org/10.1039/D1SE00918D
24. Dong R, Yan J, Ma H, Fang Y, Hao J (2011) Dimensional architecture of ferrocenyl-based oligomer honeycomb-patterned films: from monolayer to multilayer. Langmuir 27(14):9052–9056. https://doi.org/10.1021/la201264u